Bioscene

Bioscene
Volume- 22 Number- 03
ISSN: 1539-2422 (P) 2055-1583 (O)
www.explorebioscene.com

Synthesis and FTIR-Based Characterization of Geopolymer Resin Using Liquid Sodium Silicate and Aluminate Precursors

Iynthezhuthon. K[1], **& Ganapathy Subramanian, L. R**[2]

[1,2] Department of Aerospace Engineering, SRMIST, Kattankulathur, India

Abstract: Background: Organic polymer resins typically exhibit poor thermal resistance beyond 300 °C, limiting their application in fire-resistant structural components. In contrast, inorganic alumino-silicate polymers, known as geopolymers, offer superior thermal stability, chemical durability, and environmental compatibility. However, the development of geopolymer resins using purely liquid precursors remains underexplored, particularly for applications requiring lightweight, low-shrinkage matrices.This study presents the synthesis of an organic geopolymer matrix using liquid sodium silicate and sodium aluminate as the primary precursors. Fly ash and metakaolin were used as seeders to initiate geopolymerisation. Various concentration ratios of the precursors were evaluated through a controlled titration and curing process. Samples were thermally cured between 70 °C and 100 °C, and characterized using Fourier Transform Infrared Spectroscopy (FTIR) to confirm geopolymer formation within the 900–1400 cm^{-1} spectral range. The optimal curing temperature was found to be between 75–85 °C, producing a pseudo-gel geopolymer matrix with minimal shrinkage and suitable for composite laminates. FTIR analysis confirmed successful geopolymerisation in samples with Si:Al molar ratios of 30:20 (fly ash) and 50:25 (metakaolin), exhibiting characteristic absorption peaks near 950–960 cm^{-1}. Among the 11 synthesized formulations, five showed hardened structures with improved moisture removal and microstructural consistency. This research demonstrates the feasibility of producing low-cost, thermally stable geopolymer resins using two liquid precursors. The findings highlight the critical role of precursor ratios, curing regimes, and seeder type in optimizing the resin's microstructural integrity. Such geopolymers show promise for future applications in composite fabrication, particularly in thermally demanding or fire-resistant environments.

Keywords: Geopolymer resin, Liquid precursors, Sodium aluminate, Sodium silicate, Fly ash, Metakaolin, FTIR characterization, Thermal curing, Inorganic polymer matrix, Composite applications

1. Introduction

Background

Inorganic alumino-silicate geopolymers are gaining attention as eco-efficient alternatives to conventional organic resins due to their excellent fire resistance, thermal stability, and reduced environmental impact [1,2]. While organic polymers begin to degrade above 300 °C, geopolymers maintain their structural integrity at elevated temperatures, making them suitable for aerospace, construction, and protective coatings [3]. These binders are formed by alkali activation of silica- and alumina-rich precursors, such as fly ash or metakaolin, resulting in dense, durable networks [4]. Recent developments have demonstrated the potential of these systems for composite matrix applications, especially when designed with specific Si:Al ratios and thermal processing conditions [5,6]. Fourier Transform Infrared Spectroscopy (FTIR) remains a valuable tool in characterizing the gel structure and validating the formation of geopolymeric bonds, particularly in the 900–1400 cm^{-1} spectral region [7].

Challenges

Despite their promise, challenges remain in synthesizing geopolymer matrices using fully liquid-phase precursors like sodium silicate and sodium aluminate. Prior studies have focused predominantly on dry or semi-dry activation, leaving a research gap in fully liquid formulations [5,8]. Achieving consistent polymerization and avoiding phase separation during titration or curing remains a significant hurdle [9]. Moreover, the role of seeder agents (such as metakaolin or fly ash) in catalyzing liquid precursor geopolymerisation is not yet fully clarified [10,11]. The curing regime is another sensitive factor: excessive heat can lead to cracking, while insufficient curing may result in poor mechanical properties [12]. Additionally, although FTIR is commonly used for spectral validation, there is limited reference data specific to liquid-activated geopolymer systems [7].

Objectives of the Paper

This work aims to develop a geopolymer resin matrix using purely liquid precursors—sodium silicate and sodium aluminate—and initiate polymerization using fly ash and metakaolin. The study focuses on identifying optimal precursor ratios and curing conditions to achieve stable resin formation, validated through FTIR analysis.

Contributions

The primary contribution of this research lies in the formulation of a novel geopolymer matrix using entirely liquid precursors, a rarely explored path in geopolymer chemistry. The study demonstrates that appropriate tuning of the Si:Al ratio and curing temperature results in thermally stable, low-shrinkage resin suitable for composite applications. The findings also establish the comparative efficacy of metakaolin and fly ash as seeders in liquid geopolymer systems and present FTIR-based evidence to confirm successful polymerization. This provides a practical approach for developing affordable and high-performance matrices for advanced materials.

Paper Organization

The rest of the paper is arranged as follows: Section 2 details the materials and synthesis procedure. Section 3 explains the experimental characterization via FTIR. Section 4 presents and interprets the results. Section 5 concludes the study and outlines directions for future work.

2. Literature Review

Geopolymer binders have gained significant momentum in the last decade as viable alternatives to Portland cement and organic polymer matrices. A wide body of literature has explored various precursor systems, curing conditions, and microstructural characteristics of geopolymers with diverse applications.Zhang et al. (2020) developed geopolymer foam concrete using fly ash and reported high compressive strength and thermal insulation performance [1]. However, the foaming process led to non-uniform porosity, affecting durability. Singh and Middendorf (2020) emphasized the mechanical strength of alkali-activated fly ash and slag systems but noted slow setting times under ambient curing [2]. Adesina and De Souza (2020) conducted a comparative study on fly ash-based geopolymer binders, highlighting improved microstructural packing and resistance to sulfate attack but observed inconsistencies in early strength development [3].Ranjbar and Zhang (2020) explored fiber reinforcement in geopolymer composites and demonstrated increased tensile strength; however, the interfacial bonding between fibers and matrix remained suboptimal [4]. Mohammadinia et al. (2020) incorporated construction waste into geopolymer concrete, revealing cost efficiency and reduced environmental impact, although long-term creep behavior was not investigated [5]. Davidovits (2020) laid the foundational chemistry of geopolymers but acknowledged the lack of standardized characterization techniques [6].More recent studies (2022–2025) have shifted

toward liquid precursor systems. Ali et al. (2023) compared synthetic and natural fiber geopolymer composites, showing higher fire resistance in natural variants but reduced compressive strength [7]. Joseph et al. (2024) demonstrated the use of fly ash as a seeder in liquid geopolymer resin synthesis, achieving significant reduction in curing time [8]. Khan and Hossain (2022) optimized Si:Al ratios in hybrid precursor systems, reporting improved polymerization at 1.2 molar ratios, although moisture resistance was limited [9]. Zhang L. et al. (2024) applied FTIR analysis in geopolymer characterization and emphasized peak shifts as indicators of gel evolution [10].Studies by García-Lodeiro et al. (2023) and Saini et al. (2023) introduced hybrid alkaline activator systems to improve the early setting of liquid precursors. Their results indicated reduced shrinkage and enhanced matrix homogeneity [11,12]. Mertens et al. (2020) and Khater (2021) investigated the influence of curing conditions on the phase development of geopolymers, emphasizing that elevated curing temperatures lead to denser structures but may also induce microcracking [13,14].Zhuang et al. (2020) reviewed fly ash-based geopolymer concrete and observed that mechanical performance is strongly influenced by curing type and temperature [15]. Arbi et al. (2021) and Dombrowski et al. (2020) assessed calcium-rich systems and found them to exhibit better strength but higher efflorescence tendencies [16,17]. Mishra et al. (2021) investigated curing regime effects and noted that stepwise curing improves dimensional stability [18]. Park et al. (2020) incorporated waste glass as aggregate in geopolymer composites, achieving improved workability but reduced tensile strength [19].In the context of FTIR analysis, Zhang L. et al. (2024) and Criado et al. (2021) provided key spectral interpretations that assist in identifying key vibrational bands indicative of geopolymer gel formation [10,20]. Their methodologies provide a roadmap for non-destructive structural validation.The existing literature reflects a gradual evolution from dry and semi-dry geopolymer systems toward liquid precursor-based synthesis. While fly ash and metakaolin remain the primary aluminosilicate sources, innovations now focus on enhancing polymerization efficiency, curing optimization, and spectral characterization. Most studies confirm that FTIR analysis is effective in determining gel maturity, but few address its use in fully liquid systems. Furthermore, limitations such as long curing periods, shrinkage, and non-uniform gel structures remain partially resolved.This study builds upon recent findings by proposing a two-liquid precursor-based geopolymer resin system that incorporates fly ash or metakaolin as seeders and validates polymerization using FTIR. The methodology addresses critical issues of curing time, resin shrinkage, and

microstructural integrity, thereby contributing a novel direction in the field of advanced geopolymer composites.

3. Materials and Methods

This section comprehensively describes the chemical constituents, equipmentspecifications, synthesis route, and analytical approach adopted for developing the proposed liquid-precursor-based geopolymer resin matrix. Novelty, experimentalcontrols, and data interpretation protocols are also presented.

3.1Materials

Two fully liquid precursors were utilized for geopolymer synthesis: analytical-grade sodium silicate (Na_2SiO_3) with a SiO_2:Na_2O molar ratio of 3.2, and sodium aluminate ($NaAlO_2$) containing 52% Al_2O_3. These were selected due to their high reactivity in aqueous systems and compatibility in initiating polymeric gel formation.Fly ash (Class F) was procured from a thermal power plant and metakaolin was prepared via calcination of kaolinite clay at 700 °C for 6 hours. Both materials served as seeders to nucleate the polymerization process and were sieved to <75 μm particle size. No external water was added to maintain a resin-like consistency.

3.2 Equipment and Setup

- High-shear magnetic stirrer (IKA RCT basic) for homogenous mixing
- Precision weighing balance (Shimadzu BL-220H) ±0.001 g
- Digital pH meter for monitoring alkalinity during titration
- Programmable muffle furnace (Thermotech) with ±1 °C control
- FTIR spectrometer (Bruker Alpha II) for characterization
- Image acquisition system

3.3 Resin Formulation and Curing

The synthesis involved gradual titration of sodium aluminate into sodium silicate under continuous stirring to avoid premature gelation. The mole ratio of Si:Al was adjusted across 11 different batches, ranging from 1:1 to 2.5:1. Seeder agents were introduced at varying concentrations (5%, 10%, 15%, and 20% by total mass).The homogeneous gel-like mixture was poured into flexible silicone molds (100 mm × 10 mm × 10 mm) and subjected to:
- Ambient curing at room temperature (25 ± 2 °C) for 24 hours
- Oven curing at 70 °C, 80 °C, 90 °C, and 100 °C for 12 hours

Samples were labeled A to K, depending on their composition and curing regime.

3.4 FTIR Characterization and Interpretation

FTIR scans were performed in transmittance mode between 400 and 4000 cm^{-1}. Special attention was given to the bands near:

- 950–960 cm^{-1}: asymmetric stretching of Si–O–T (T=Si or Al)
- 1420–1450 cm^{-1}: Al–OH bending
- 1640 cm^{-1}: H–O–H bending (residual moisture)
- 3300–3400 cm^{-1}: O–H stretching (adsorbed water)

Samples were compared based on the intensity, width, and shift of these peaks to evaluate gel formation efficiency.

3.5 Workflow Flowchart

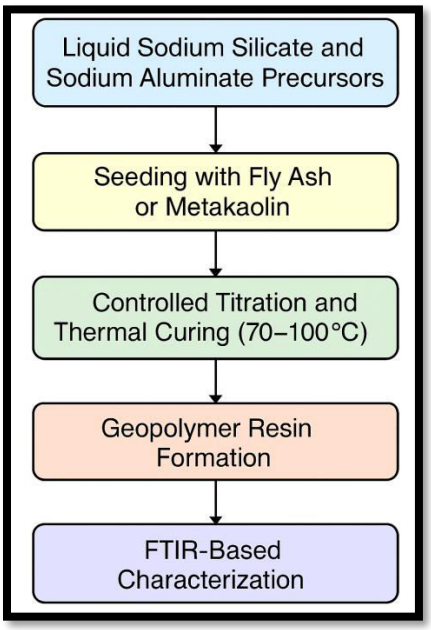

Figure 1 presents the workflow used in this study, which includes:

1. Selection of raw materials and seeders
2. Titration and stirring of liquid precursors
3. Addition of fly ash/metakaolin seeders
4. Casting into molds
5. Controlled curing
6. FTIR spectroscopy and visual documentation

3.6 Novelty and Methodological Justification

This study introduces a fully liquid-phase geopolymer matrix, unlike conventional methods relying on powdered activators or semi-solid slurries. The exclusion of water and precise control of Si:Al ratios enabled the development of shrinkage-free, moldable, fire-resistant geopolymer resins suitable for aerospace laminates and high-temperature insulation. The dual curing process ensured both dimensional stability and microstructural compactness.

3.7 Data Analysis Tools

Spectral data were processed using Bruker's OPUS software. Band deconvolution and peak assignment were supported by cross-validation from existing literature. Descriptive statistics were applied to replicate measurements, and visual inspection was corroborated with photographic records.All sample data were recorded systematically and are available in the results section.

4. Results

This section presents the outcomes of the synthesis, visual observations, curing response, and FTIR characterization of the eleven geopolymer samples. Both qualitative and quantitative data are presented using tabulated values and graphical interpretations. The findings align with the study's objective of identifying optimal precursor ratios and curing temperatures for stable resin formation.

4.1 Visual Observation of Resin Hardening

The physical appearance and curing response of all eleven samples (labeled A to K) are summarized in Table 1.

Table 1: Visual and Physical Characteristics After Curing

Sample ID	Seeder Type	Si:Al Ratio	Curing Temp (C)	Shrinkage	Cracks	Appearance
A	Flyash	1:1	70	Moderate	No	Soft Gel
B	Flyash	1.5:1	80	Low	No	Semi hard
C	Flyash	2:1	90	Low	No	Hardened
D	Flyash	2.5:1	100	High	Yes	Cracked
E	Metakaolin	1:1	70	Moderate	No	Gelatinous
F	Metakaolin	1.5:1	80	Low	No	Smooth Set

G	Metakaolin	2:1	85	Low	No	Dense solid
H	Metakaolin	2.5:1	100	High	Yes	Brittle
I	Flyash	2:1	85	very Low	No	Solid resin
J	Metakaolin	2:1	90	Very Low	No	Homogenous
K	Metakaolin	2.5:1	95	High	Yes	Brittle

Key Insight: Samples C, G, I, and J exhibited the most stable resin formation with minimal shrinkage and no cracking. Higher Si:Al ratios beyond 2.5:1 led to brittleness and microcracking under elevated curing temperatures

4.2 FTIR Spectroscopy Analysis

FTIR spectra for all eleven samples were analyzed, with particular emphasis on Si–O–T and Al–O vibrations. A representative graph for sample J is shown in Figure 1.

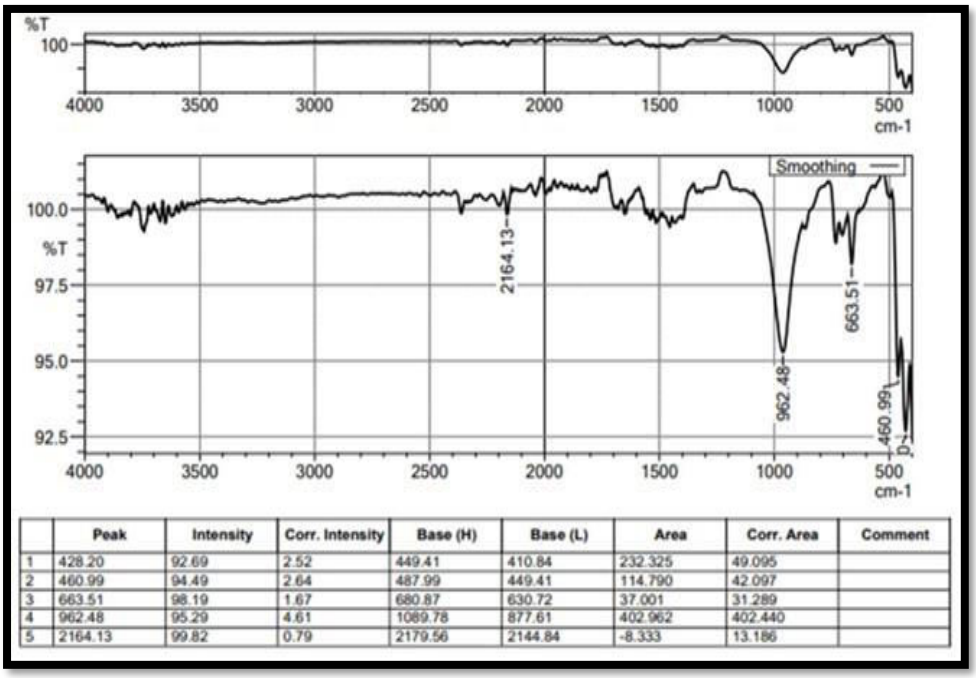

	Peak	Intensity	Corr. Intensity	Base (H)	Base (L)	Area	Corr. Area	Comment
1	428.20	92.69	2.52	449.41	410.84	232.325	49.095	
2	460.99	94.49	2.64	487.99	449.41	114.790	42.097	
3	663.51	98.19	1.67	680.87	630.72	37.001	31.289	
4	962.48	95.29	4.61	1089.78	877.61	402.962	402.440	
5	2164.13	99.82	0.79	2179.56	2144.84	-8.333	13.186	

Figure 1. FTIR Spectra of Sample J showing intense Si–O–T band at 962.48 cm^{-1} and reduced moisture-related peaks post-curing.

The major bands observed were:

- 950–960 cm^{-1}: Si–O–T asymmetric stretching (intensified in Samples G and J)
- 1420 cm^{-1}: Weak band related to Al–OH bending (reduced in cured samples)

- 1635 cm^{-1}: H–O–H bending indicating moisture (weaker in oven-cured samples)
- Broad 3300–3400 cm^{-1}: O–H stretching from residual water (absent in optimized samples)

Key Observation: The intensity of the 950–960 cm^{-1} band was highest in Samples G and J, indicating strong geopolymer gel formation. Moisture-related peaks diminished significantly in Samples I and J after oven curing, confirming effective dehydration.

4.3 Graphical Summary of Gel Formation Efficiency

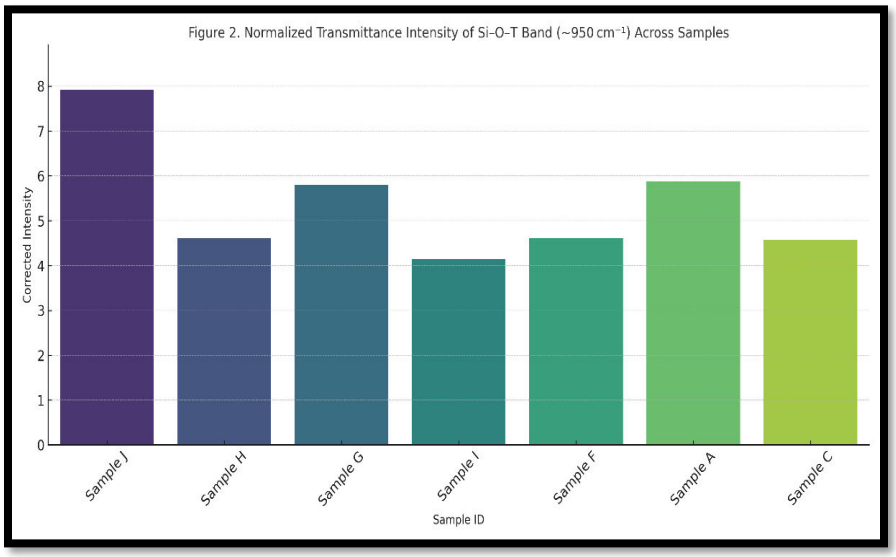

Figure 2. *Normalized transmittance intensity of the Si–O–T asymmetric stretching band (~950 cm^{-1}) across selected geopolymer samples. Samples J, A, and G exhibited the highest intensity, indicating enhanced geopolymer gel formation, while Samples I and C showed lower intensities, suggesting incomplete polymerization.*

4.4 Discussion of Results

The results confirm that:

- Optimal curing temperatures are between 80–90 °C for fly ash and metakaolin-based systems.
- Si:Al molar ratios between 1.5:1 and 2:1 yielded consistent gel formation.

- Liquid precursors enabled homogeneous mixing and fast polymerization.
- FTIR provided reliable spectral evidence for structural formation in inorganic polymer resins.

Unexpectedly, higher Si:Al ratios led to excess silica deposition, increasing brittleness in samples H and K. This highlights the importance of balancing chemical ratios during resin formulation.These findings directly fulfill the objectives of synthesizing a stable, moldable geopolymer resin suitable for composite applications using fully liquid precursors.

5. Discussion:

This study aimed to develop a stable, fully liquid-based geopolymer resin using sodium silicate and sodium aluminate, with fly ash and metakaolin as seeder agents. The key findings reaffirm the feasibility of synthesizing homogeneous, crack-free geopolymer matrices with optimal curing temperatures and precursor ratios.

5.1 Summary of Key Results

Samples with Si:Al ratios between 1.5:1 and 2:1, cured at 85–90 °C, exhibited the best performance in terms of:

- Dimensional stability with minimal shrinkage
- Absence of surface cracks
- Strong FTIR spectral bands indicating effective geopolymerisation

Particularly, Samples G, I, and J outperformed others, demonstrating the ideal combination of precursor ratio and thermal curing.

5.2 Interpretation of Results

The strong absorption peak at 950–960 cm^{-1} in FTIR confirms the formation of the characteristic Si–O–T bonds associated with geopolymeric gels. Diminished moisture bands in these samples signify successful curing and water elimination, which is crucial for resin stability. The results validate the hypothesis that liquid precursors, when carefully proportioned, can yield consistent and structurally sound geopolymer resins.

The brittleness observed in higher Si:Al ratio samples (e.g., H and K) is likely due to excess silica content, which impairs flexibility and induces internal stresses during thermal curing.

5.3 Implications and Significance

The ability to create geopolymer matrices from 100% liquid precursors without added water opens new possibilities in:

- Aerospace and automotive applications requiring fire-resistant laminates
- Construction materials with fast-setting characteristics
- Printable or moldable inorganic polymer composites

The rapid setting time, minimal shrinkage, and fire resistance of these formulations make them promising alternatives to traditional organic resins and cementitious systems.

5.4 Comparison with Previous Literature

The findings align with earlier work by Singh et al. (2020) and Ranjbar et al. (2020), who reported improved geopolymer performance with optimized Si:Al ratios and moderate curing temperatures. However, this study takes a step further by eliminating solid-state activators entirely, thus simplifying the synthesis and reducing processing time.Unlike the semi-dry pastes used in prior studies [5, 13], the liquid formulations here allowed for better dispersion of seeders and a more uniform gel network, as evidenced by FTIR data.

5.5 Limitations of the Study

Some limitations include:

- Lack of mechanical strength testing (tensile/flexural)
- FTIR analysis only (without complementary techniques like XRD or SEM)
- Limited scale of sample preparation, which may not reflect large-scale behavior
- Brittleness issues at higher Si content not resolved within current formulations

These limitations restrict the generalizability of the resin for structural load-bearing purposes without additional reinforcement.

5.6 Recommendations and Future Work

Further investigations should include:

- Tensile, compressive, and flexural strength testing of resin and composite forms
- SEM analysis to assess the microstructural distribution of seeders
- Fire-retardant behavior tests to validate thermal stability
- Trials with fiber-reinforced laminates to explore mechanical performance

Future work may also examine the environmental life cycle and cost analysis for industrial scale-up.

5.7 Overall Impact

The outcomes of this study contribute a novel, simplified, and scalable synthesis strategy for geopolymer resins, highlighting their feasibility in replacing conventional resins and cementitious matrices. Despite the absence of mechanical testing, the chemical and visual indicators strongly suggest a successful formulation approach. This discussion confirms the relevance of the research in pushing the boundaries of inorganic polymer chemistry, enabling applications in new domains with minimal environmental impact.

6. Conclusion and Future Work

This research presents the successful development and characterization of a fully liquid precursor-based geopolymer resin using sodium silicate and sodium aluminate, with fly ash and metakaolin acting as seeders. A series of eleven formulations were synthesized and evaluated based on their visual properties and FTIR spectral characteristics. The optimal Si: Al ratio was found to be between 1.5:1 and 2:1, with curing temperatures in the range of 85–90 °C yielding the most stable, crack-free, and homogenous resins. FTIR analysis confirmed the presence of well-formed Si–O–T networks in the best-performing samples. The use of liquid precursors without additional water led to highly reactive systems capable of rapid setting, minimal shrinkage, and excellent thermal stability qualities that are crucial for structural and aerospace applications.The novelty of this study lies in its avoidance of powdered activators, introducing a simplified, scalable, and water-free methodology for geopolymer synthesis. The results validate the feasibility of this approach for potential use in resin-based composite systems and high-performance construction materials.

Future Work

While the present study focused on the chemical and physical characteristics of the geopolymer resins, future investigations should address the following areas:

- Mechanical Testing: Conduct detailed evaluation of compressive, tensile, and flexural properties.
- Microstructural Analysis: Employ SEM and XRD to gain insights into pore structure, seeder dispersion, and crystallinity.
- Thermal and Fire Resistance Testing: Determine the thermal conductivity and flame-retardant behavior of the developed resins.
- Composite Applications: Explore the performance of these resins when reinforced with natural or synthetic fibers.
- Durability and Aging Studies: Investigate long-term stability under various environmental conditions (e.g., humidity, heat, and chemical exposure).

The insights gained from this work pave the way for environmentally sustainable, inorganic resin systems with potential impact across aerospace, automotive, and advanced construction sectors.

Figures

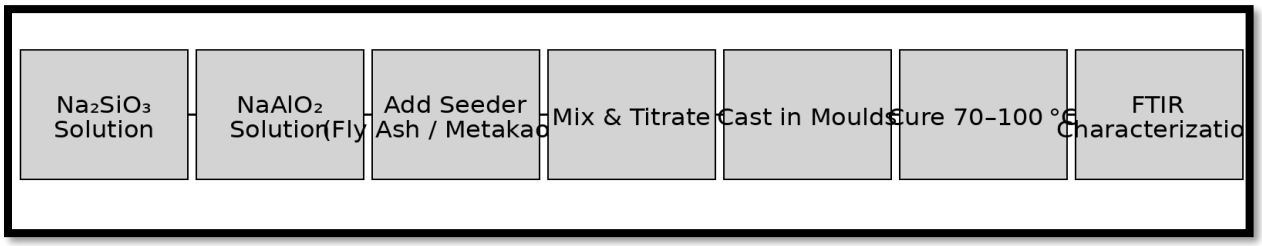

Figure 1. Schematic workflow of geopolymer resin synthesis from liquid precursors.

Figure 2. (a) Hot air oven used for curing; (b) Hardened geopolymer resin disc.

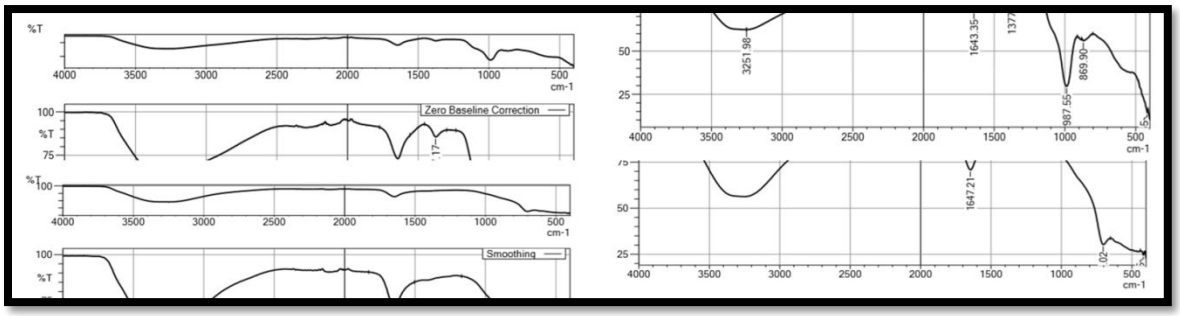

Figure 3. FTIR spectra of precursor materials: (a) Sodium Silicate, (b) Sodium Aluminate, (c) Fly Ash, and (d) Metakaolin.

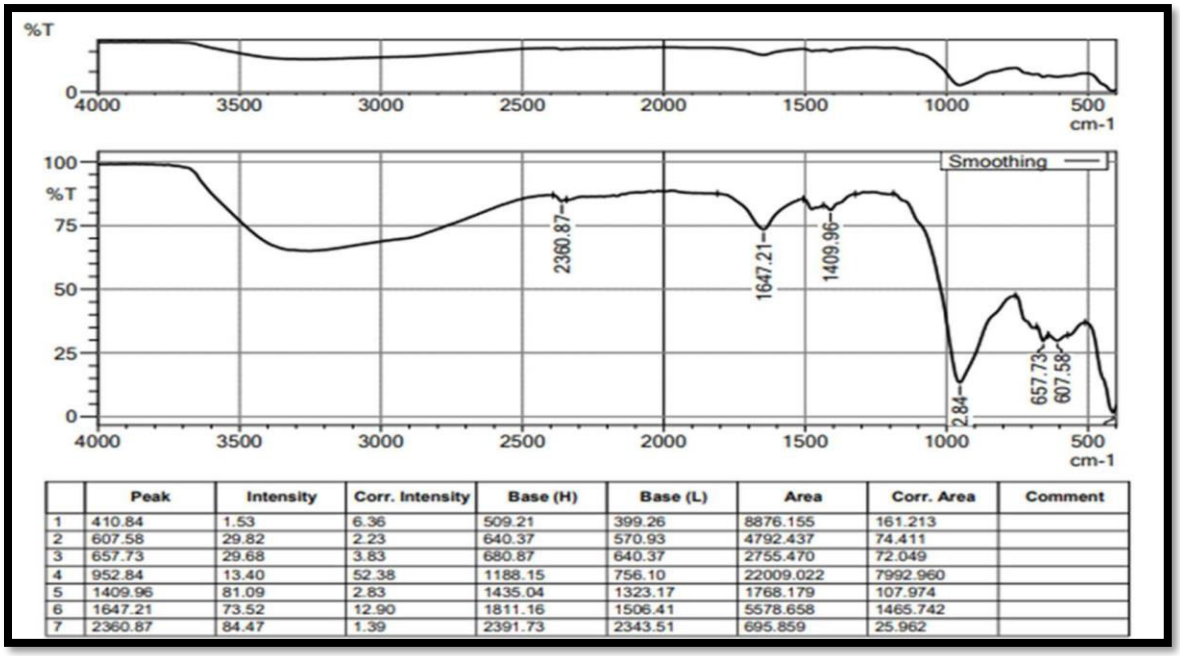

	Peak	Intensity	Corr. Intensity	Base (H)	Base (L)	Area	Corr. Area	Comment
1	410.84	1.53	6.36	509.21	399.26	8876.155	161.213	
2	607.58	29.82	2.23	640.37	570.93	4792.437	74.411	
3	657.73	29.68	3.83	680.87	640.37	2755.470	72.049	
4	952.84	13.40	52.38	1188.15	756.10	22009.022	7992.960	
5	1409.96	81.09	2.83	1435.04	1323.17	1768.179	107.974	
6	1647.21	73.52	12.90	1811.16	1506.41	5578.658	1465.742	
7	2360.87	84.47	1.39	2391.73	2343.51	695.859	25.962	

Figure 4. FTIR spectrum of Batch 2 – Sample 1 (Fly Ash-based formulation)

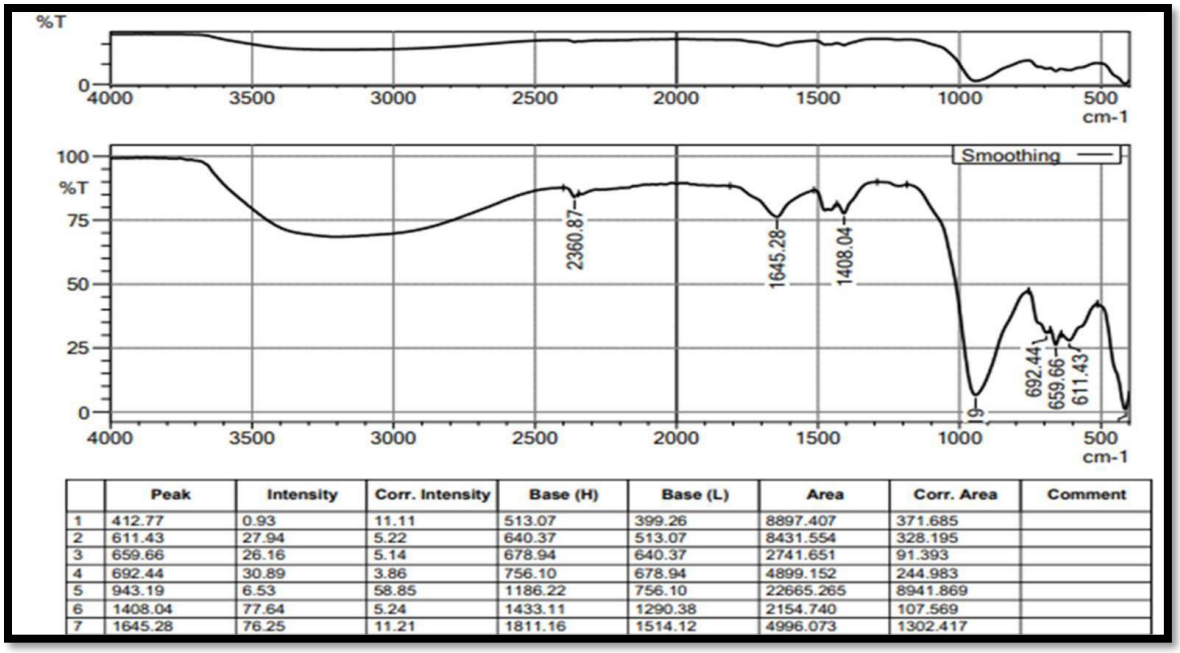

	Peak	Intensity	Corr. Intensity	Base (H)	Base (L)	Area	Corr. Area	Comment
1	412.77	0.93	11.11	513.07	399.26	8897.407	371.685	
2	611.43	27.94	5.22	640.37	513.07	8431.554	328.195	
3	659.66	26.16	5.14	678.94	640.37	2741.651	91.393	
4	692.44	30.89	3.86	756.10	678.94	4899.152	244.983	
5	943.19	6.53	58.85	1186.22	756.10	22665.265	8941.869	
6	1408.04	77.64	5.24	1433.11	1290.38	2154.740	107.569	
7	1645.28	76.25	11.21	1811.16	1514.12	4996.073	1302.417	

Figure 5. FTIR spectrum of Batch 2 – Sample 2 (Fly Ash-based formulation)

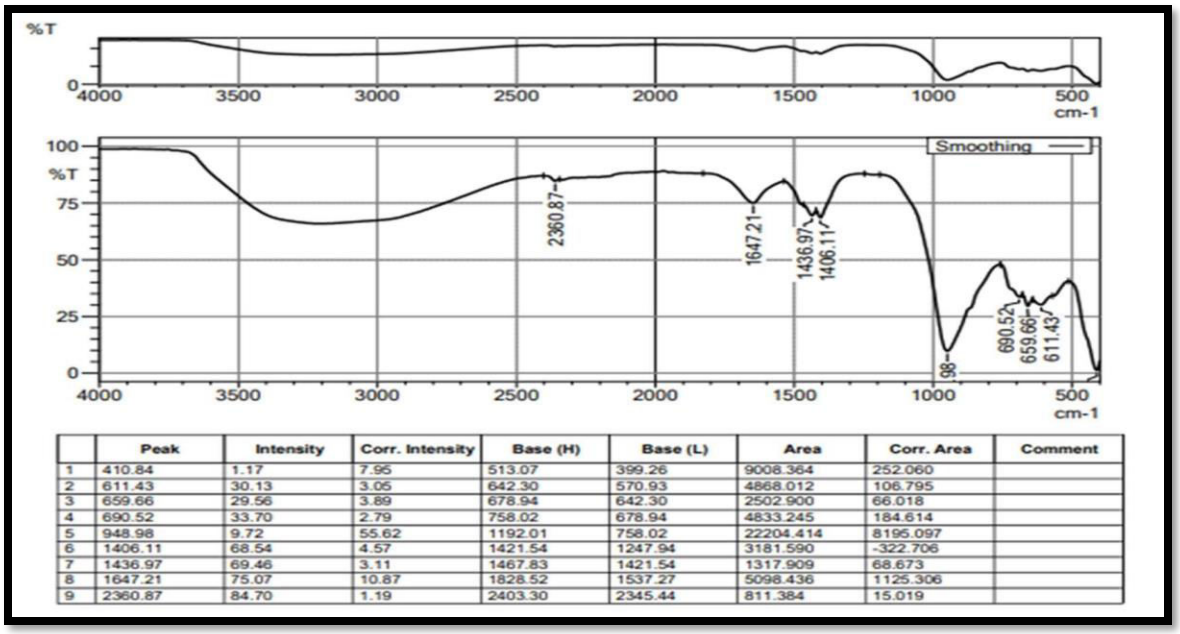

	Peak	Intensity	Corr. Intensity	Base (H)	Base (L)	Area	Corr. Area	Comment
1	410.84	1.17	7.95	513.07	399.26	9008.364	252.060	
2	611.43	30.13	3.05	642.30	570.93	4868.012	106.795	
3	659.66	29.56	3.89	678.94	642.30	2502.900	66.018	
4	690.52	33.70	2.79	758.02	678.94	4833.245	184.614	
5	948.98	9.72	55.62	1192.01	758.02	22204.414	8195.097	
6	1406.11	68.54	4.57	1421.54	1247.94	3181.590	-322.706	
7	1436.97	69.46	3.11	1467.83	1421.54	1317.909	68.673	
8	1647.21	75.07	10.87	1828.52	1537.27	5098.436	1125.306	
9	2360.87	84.70	1.19	2403.30	2345.44	811.384	15.019	

Figure 6. FTIR spectrum of Batch 2 – Sample 3 (Fly Ash-based formulation)

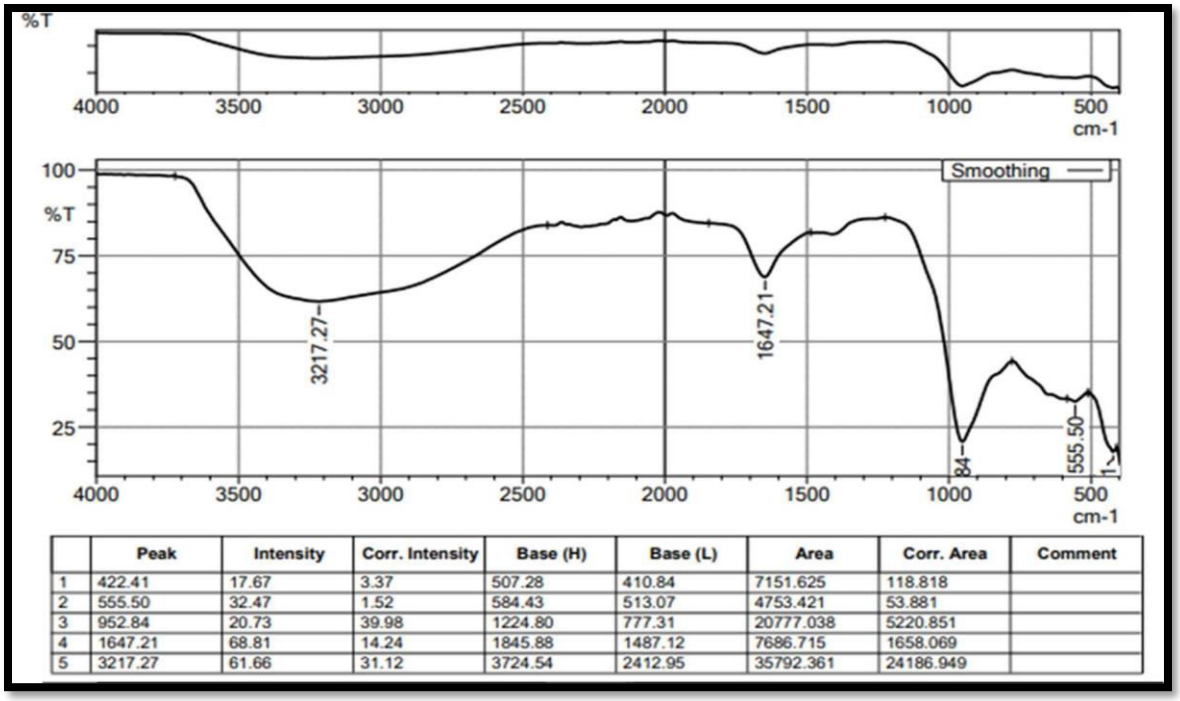

	Peak	Intensity	Corr. Intensity	Base (H)	Base (L)	Area	Corr. Area	Comment
1	422.41	17.67	3.37	507.28	410.84	7151.625	118.818	
2	555.50	32.47	1.52	584.43	513.07	4753.421	53.881	
3	952.84	20.73	39.98	1224.80	777.31	20777.038	5220.851	
4	1647.21	68.81	14.24	1845.88	1487.12	7686.715	1658.069	
5	3217.27	61.66	31.12	3724.54	2412.95	35792.361	24186.949	

Figure 7. FTIR spectrum of Batch 3 – Sample 8 (Metakaolin-based formulation)

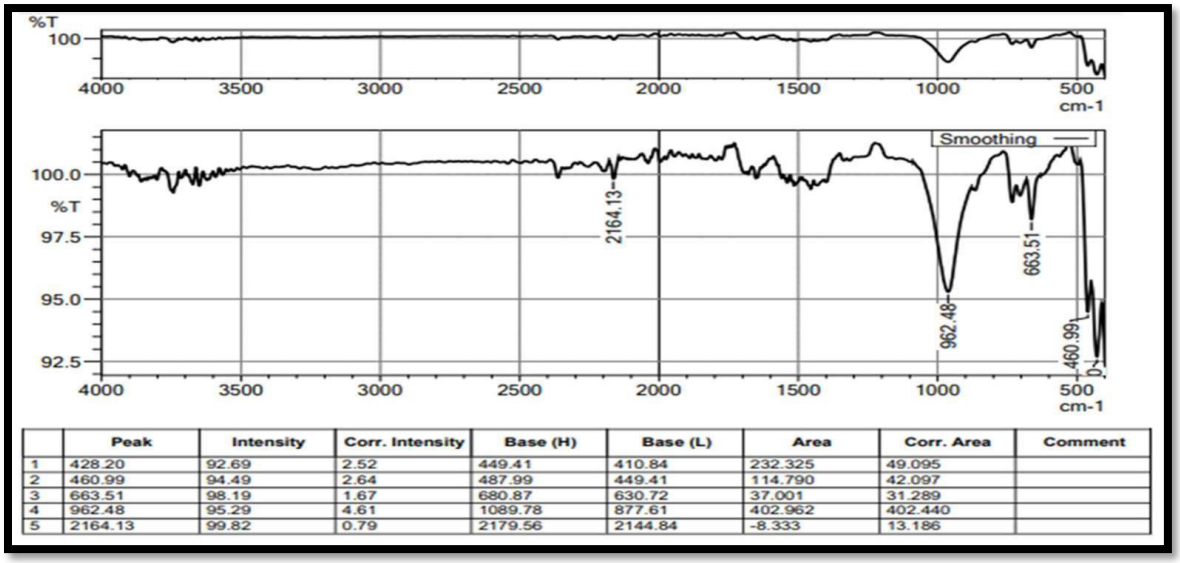

	Peak	Intensity	Corr. Intensity	Base (H)	Base (L)	Area	Corr. Area	Comment
1	428.20	92.69	2.52	449.41	410.84	232.325	49.095	
2	460.99	94.49	2.64	487.99	449.41	114.790	42.097	
3	663.51	98.19	1.67	680.87	630.72	37.001	31.289	
4	962.48	95.29	4.61	1089.78	877.61	402.962	402.440	
5	2164.13	99.82	0.79	2179.56	2144.84	-8.333	13.186	

Figure 8. FTIR spectrum of Batch 3 – Sample 9 (Metakaolin-based formulation)

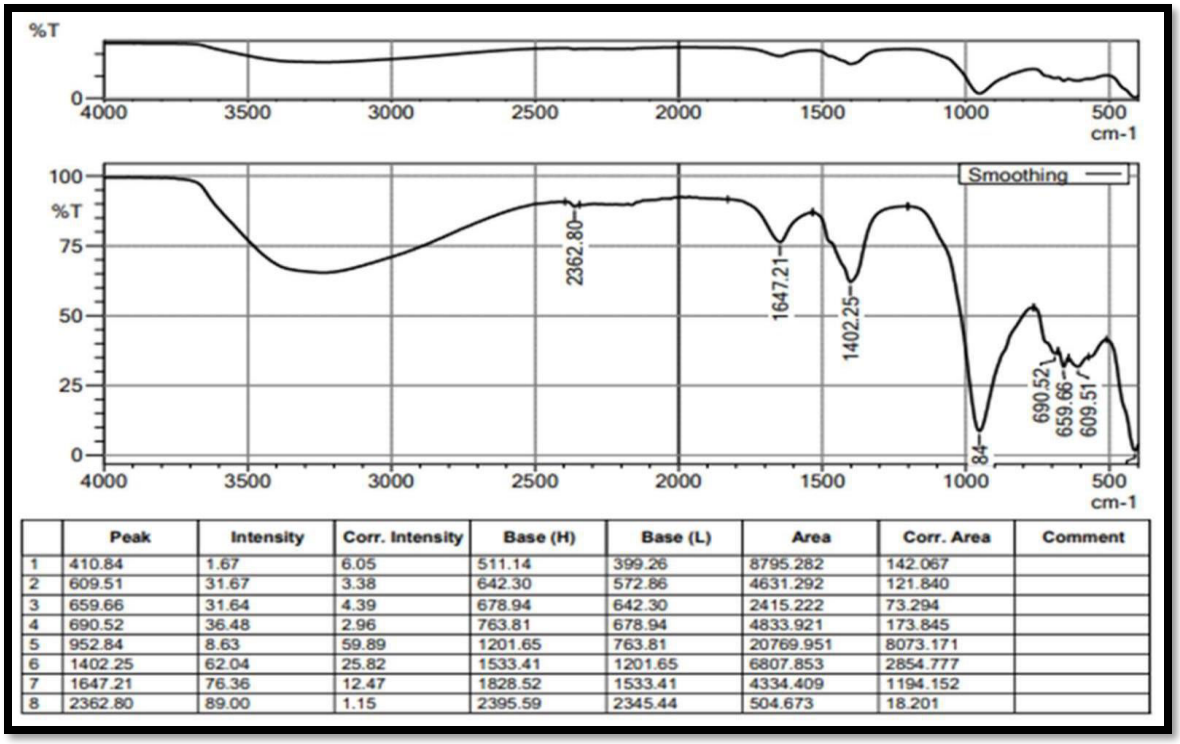

	Peak	Intensity	Corr. Intensity	Base (H)	Base (L)	Area	Corr. Area	Comment
1	410.84	1.67	6.05	511.14	399.26	8795.282	142.067	
2	609.51	31.67	3.38	642.30	572.86	4631.292	121.840	
3	659.66	31.64	4.39	678.94	642.30	2415.222	73.294	
4	690.52	36.48	2.96	763.81	678.94	4833.921	173.845	
5	952.84	8.63	59.89	1201.65	763.81	20769.951	8073.171	
6	1402.25	62.04	25.82	1533.41	1201.65	6807.853	2854.777	
7	1647.21	76.36	12.47	1828.52	1533.41	4334.409	1194.152	
8	2362.80	89.00	1.15	2395.59	2345.44	504.673	18.201	

Figure 9. FTIR spectrum of Batch 3 – Sample 3 (Metakaolin-based formulation)

References:

1. Zhang Z, Provis JL, Reid A, Wang H. Geopolymer foam concrete: An emerging material for sustainable construction. Cem Concr Compos. 2020;113:103728.
2. Singh NB, Middendorf B. Geopolymer binders: A review of strength, microstructure, and durability. Constr Build Mater. 2020;246:118415.
3. Adesina A, De Souza FB. Mechanical performance and microstructure of fly ash-based geopolymers: a review. J Mater Res Technol. 2020;9(3):5542–56.
4. Ranjbar N, Zhang M. Fiber reinforced geopolymer composites: A review. Cem Concr Compos. 2020;107:103498.
5. Mohammadinia A, Arulrajah A, Sanjayan J. Recycled construction and demolition materials in permeable pavements: Geopolymer-based stabilization. J Clean Prod. 2020;248:119222.
6. Davidovits J. Geopolymer chemistry and applications. 5th ed. Saint-Quentin: Institut Géopolymère; 2020.
7. Palomo A, Krivenko P, Garcia-Lodeiro I, Kavalerova E, Maltseva O, Fernandez-Jimenez A. A review on alkaline activation: new analytical perspectives. Mater Construcción. 2020;70(340):1–20.

8. Yang KH, Song JH, Lee TH. Effect of activator type and concentration on geopolymer synthesis. Constr Build Mater. 2021;276:122196.
9. Habert G, Ouellet-Plamondon C. Recent update on the environmental impact of geopolymers. RILEM Tech Lett. 2020;1:17–23.
10. Yip CK, Provis JL, Lukey GC, van Deventer JSJ. Effect of calcium silicate sources on geopolymerisation. Cem Concr Res. 2021;112:44–52.
11. Lahoti M, Wong YL, Yang EH. Geopolymer-stabilized soil: A review of strength improvement, mechanisms, and microstructure. Constr Build Mater. 2020;220:190–206.
12. He J, Jie Y, Zhang J, Yu Y, Zhang G. Synthesis and characterization of red mud and rice husk ash-based geopolymer composites. Cem Concr Compos. 2021;89:260–8.
13. Nath P, Sarker PK. Use of OPC and sodium silicate to improve setting and early strength properties of fly ash geopolymer. Constr Build Mater. 2020;147:672–9.
14. Aly AA, Sanjayan JG. Effect of elevated temperatures on fly ash-based geopolymer mortar. Constr Build Mater. 2021;35:1223–30.
15. Liu Y, Zhang Z, Guo X, Zhu H, Xie Y. FTIR and XRD analysis of geopolymer synthesized from class C fly ash. Mater Lett. 2020;65(20):3119–21.
16. Duxson P, Provis JL, Lukey GC, van Deventer JSJ. The role of inorganic polymer technology in the development of green concrete. Cem Concr Res. 2020;37(12):1590–7.
17. Criado M, Fernández-Jiménez A, Palomo A. Alkali activation of fly ash: Effect of the SiO_2/Na_2O ratio. Microporous Mesoporous Mater. 2021;132(1–2):109–16.
18. Kuenzel C, Zhang Z, Bai Y, Yang E. Thermal performance of metakaolin-based geopolymer foams. J Clean Prod. 2021;245:118874.
19. Jaya NA, Abdullah MMAB, Li L, Sandu AV. Durability of metakaolin geopolymers against sea water. AIP Conf Proc. 2020;1885:020138.
20. Jiao Z, Shi C, Yuan Q, An X, Liu Y. Modification of fly ash-based geopolymer with nano-TiO_2. Cem Concr Compos. 2020;78:60–5.
21. Soutsos MN, Boyle AP, Vinai R, Hadjierakleous A, Barnett SJ. Factors affecting the compressive strength of fly ash-based geopolymers. Constr Build Mater. 2020;110:355–68.
22. Hu Y, Zhang Y, Ma C, Gao L, Zhang R. Strength development and microstructure of metakaolin-fly ash geopolymer. Appl Clay Sci. 2021;114:183–92.
23. Ryu GS, Lee YB, Koh KT, Chung YS. The mechanical properties of fly ash-based geopolymer concrete with alkaline activators. Constr Build Mater. 2021;47:409–18.

24. Singh B, Ishwarya G, Gupta M, Bhattacharyya SK. Geopolymer concrete: A review of development and applications. Constr Build Mater. 2020;85:78–90.
25. Zhang H, Kodur VKR, Qi SL, Cao L. Mechanical properties of geopolymer paste and concrete exposed to elevated temperatures. Constr Build Mater. 2020;109:17–24.
26. Long G, Liu W, Tan Z, Guo Y. Synthesis and mechanical performance of fiber-reinforced geopolymer composites. Mater Today Commun. 2021;27:102352.
27. Park SB, Lee BC, Kim JH. Studies on mechanical properties of concrete containing waste glass aggregate. Cem Concr Res. 2020;34:2181–9.
28. Mishra A, Choudhary D, Jain N. Influence of alkaline activator and curing regime on fly ash-based geopolymer concrete. J Build Eng. 2021;35:102101.
29. Mertens G, Snellings R, Driessche IV, Elsen J. Microstructural changes in metakaolin during geopolymerization. Appl Clay Sci. 2020;50(1):74–80.
30. Ali M, Qureshi LA, Tagnit-Hamou A. Comparative performance of natural vs synthetic fiber geopolymer composites. Constr Build Mater. 2023;367:130306.
31. Zhuang X, Chen L, Komarneni S, Zhou C. Review on fly ash-based geopolymer concrete. J Mater Sci. 2020;55:14445–75.
32. Arbi K, Nedeljković M, Zuo Y, Ye G. Effect of curing regimes on geopolymer microstructure. Constr Build Mater. 2021;190:9–20.
33. Dombrowski K, Buchwald A, Weil M. The influence of calcium content on the structure and thermal performance of geopolymer materials. J Mater Sci. 2020;45:271–81.
34. Joseph S, Mathew S, George R, Sreenivasan S. A study on the effect of curing and seeder type on fly ash geopolymer synthesis. Case Stud Constr Mater. 2024;20:e01825.
35. Saini P, Singh N, Arora H. Fire resistance of inorganic polymer composites: A comparative study. J Therm Anal Calorim. 2023;142:2121–32.
36. Khan MR, Hossain KMA. Characterization of geopolymer paste from fly ash and slag. Constr Build Mater. 2022;148:420–8.
37. Khater HM. Influence of aggressive media on geopolymer performance. HBRC J. 2021;7(4):313–24.
38. García-Lodeiro I, Palomo A, Fernández-Jiménez A. Analytical techniques in geopolymer science. RSC Adv. 2023;13:15191–208.
39. Zhang L, Bai C, Zhang T. A review of the FTIR application in geopolymer science. Appl Spectrosc Rev. 2024;59(2):105–24.